Human GLTP: Three Distinct Functions for the Three Tryptophans in a Novel Peripheral Amphitropic Fold

Ravi Kanth Kamlekar,[†] Yongguang Gao,[†] Roopa Kenoth,[†] Julian G. Molotkovsky,[‡] Franklyn G. Prendergast,[§] Lucy Malinina,[¶] Dinshaw J. Patel,[‖] William S. Wessels,[§] Sergei Y. Venyaminov,[§] and Rhoderick E. Brown[†*]

[†]The Hormel Institute, University of Minnesota, Austin, Minnesota; [‡]Shemyakin and Ovchinnikov Institute of Bioorganic Chemistry, Russian Academy of Sciences, Moscow, Russia; [§]Mayo Clinic College of Medicine, Rochester, Minnesota; [¶]Structural Biology, Centro de Investigación Cooperativa BioGUNE, Derio, Spain; and [‖]Structural Biology Program, Memorial Sloan-Kettering Cancer Center, New York, New York

ABSTRACT Human glycolipid transfer protein (GLTP) serves as the GLTP-fold prototype, a novel, to our knowledge, peripheral amphitropic fold and structurally unique lipid binding motif that defines the GLTP superfamily. Despite conservation of all three intrinsic Trps in vertebrate GLTPs, the Trp functional role(s) remains unclear. Herein, the issue is addressed using circular dichroism and fluorescence spectroscopy along with an atypical Trp point mutation strategy. Far-ultraviolet and near-ultraviolet circular dichroism spectroscopic analyses showed that W96F-W142Y-GLTP and W96Y-GLTP retain their native conformation and stability, whereas W85Y-W96F-GLTP is slightly altered, in agreement with relative glycolipid transfer activities of >90%, ~85%, and ~45%, respectively. In silico three-dimensional modeling and acrylamide quenching of Trp fluorescence supported a nativelike folding conformation. With the Trp^{96}-less mutants, changes in emission intensity, wavelength maximum, lifetime, and time-resolved anisotropy decay induced by phosphoglyceride membranes lacking or containing glycolipid and by excitation at different wavelengths along the absorption-spectrum red edge indicated differing functions for W142 and W85. The data suggest that W142 acts as a shallow-penetration anchor during docking with membrane interfaces, whereas the buried W85 indole helps maintain proper folding and possibly regulates membrane-induced transitioning to a glycolipid-acquiring conformation. The findings illustrate remarkable versatility for Trp, providing three distinct intramolecular functions in the novel amphitropic GLTP fold.

INTRODUCTION

Glycolipid transfer protein (GLTP) was initially discovered in the membrane-free cytosolic extract of bovine spleen because of its ability to selectively accelerate the intermembrane transfer of glycolipids ((1) and references therein). Proteins with similar activity subsequently were found in a wide variety of tissues. GLTPs (~209 amino acids) are highly conserved among mammals, show high specificity toward glycolipids, and occur in nearly all eukaryotic cells, with the possible exception of certain unicellular yeasts (1–3). GLTP uses a distinct two-layer sandwich motif, dominated by α-helices and achieved without intramolecular disulfide bridges, to bind a single glycolipid molecule (4–6). Because of its unique conformation among lipid-binding/transfer proteins, the GLTP fold serves as the prototype for the GLTP superfamily (1,3).

The pivotal role played by GLTP-like folds in larger proteins, e.g., phosphoinositol 4-phosphate adaptor protein-2 (FAPP2), has recently become clear. FAPP2 (519 amino acids) contains a pleckstrin homology (PH) domain that binds to phosphatidylinositol 4-phosphate in the Golgi in an ADP-ribosylation-factor-dependent manner and a GLTP-like domain that enables transport of glucosylceramide (GlcCer) from its site of synthesis in the cytosolic leaflet of the Golgi complex to its site of conversion into more complex glycosphingolipids in the late Golgi compartments (7). In vivo RNAi knockdown of FAPP2-mediated GlcCer transfer fails to block the transport of newly synthesized GlcCer to the cell surface in the presence of the vesicle trafficking disruptor brefeldin A, suggesting partial redundancy of GlcCer transfer by GLTP (8). It came as no surprise that molecular modeling of the FAPP2-GLTP-like domain shows conservation of key residues involved in glycolipid transfer/binding and high folding homology with GLTP (7).

The region surrounding the glycolipid binding site of GLTP is postulated to serve as its membrane interaction domain based on the proximity of nearby tryptophans, tyrosines, and lysines (4,5,9–13). These membrane interaction residues are spatially organized within a conformational fold that differs from other known membrane interaction/docking domains associated with various peripheral and amphitropic proteins, i.e., the C1, C2, PH, PX, and FYVE domains (9,14–17). Membrane interaction by the amphitropic GLTP fold enables binding of glycolipid and formation of a soluble complex (12,18–20). Mapping of the glycolipid binding site by high-resolution structural and point-mutational studies has shown that the GLTP fold adapts to accommodate glycolipids with various sugar-headgroup and acyl structural differences (4–6,12). The crystal structures of glycolipid-free GLTP and GLTP-glycolipid complexes provide before-and-after snapshots of the protein's conformation, which is only slightly altered by

Submitted February 15, 2010, and accepted for publication August 10, 2010.

*Correspondence: rebrown@hi.umn.edu

Editor: Amitabha Chattopadhyay.

0006-3495/10/10/2626/10 $2.00

doi: 10.1016/j.bpj.2010.08.038

binding of various glycolipids (4–6). Nonetheless, interaction of GLTP with membranes containing glycolipid dramatically alters intrinsic Trp fluorescence, producing an intensity decrease (~40%) and a large blue shift (~12 nm) in emission-wavelength maximum (10,12,19). The changes in Trp fluorescence induced by interaction with membranes containing glycolipid are dominated by Trp^{96}, masking the contributions from the other two Trp residues (Trp^{85} and Trp^{142}) that also reside on/near the protein surface. To elucidate the functional role(s) played by Trp^{85} and Trp^{142}, we developed new Trp mutants of human GLTP, i.e., W96Y, W85Y-W96F, and W96F-W142Y. Fluorescence and circular dichroic spectroscopic analyses in the presence and absence of membranes containing or lacking glycolipid provide experimental evidence to support the idea that Trp^{96} and Trp^{85} play distinct and differing roles in the amphitropic GLTP fold.

MATERIALS AND METHODS

GLTP Trp mutants (W96Y, W85Y-W96F, and W96F-W142Y) were produced by QuikChange mutagenesis (Stratagene, La Jolla, CA). Measurements of glycolipid intermembrane transfer activity, circular dichroism (CD) spectroscopy, and Trp fluorescence are described in the Supporting Material.

RESULTS

Tryptophan topography in wtGLTP

X-ray diffraction and fluorescence studies have shown that all three Trp residues are located at or near the surface of human GLTP (4–6,10–13,19). W142 is completely exposed to the aqueous milieu (Fig. 1), whereas W96 forms the bottom of a surface depression, serving as a stacking platform that orients the initial ceramide-linked sugar for hydrogen bonding with Asp^{48}, Asn^{52}, and Lys^{55}. W85 is located near the protein surface, but its indole ring projects toward the interior and is sandwiched between Pro^{86} (*cis* configuration) and Lys^{78} (cation-π interaction), facilitating hydrogen bonding between the pyrrole nitrogen group and the Thr^{91} side-chain hydroxyl group. The Trps are located within or close to the glycolipid binding site, near a cluster of nonpolar residues (Fig. 1 *B*) that form a putative membrane interaction domain (4–6). To evaluate Trp functionality, active single-Trp GLTP mutants were generated using an atypical strategy involving replacement with both Phe and Tyr. Compared to wtGLTP, W96F-W142Y-GLTP and W96Y-GLTP retained >90% and ~85% activity, respectively; whereas W85Y-W96F-GLTP transfer activity decreased to ~45% (Fig. S1 in the Supporting Material). Similar outcomes were obtained using fluorescently labeled glycolipid to monitor transfer activity (data not shown).

CD spectral analysis

Far-ultraviolet (UV) CD (190–250 nm) analyses of wtGLTP showed a secondary structure dominated by α-helices

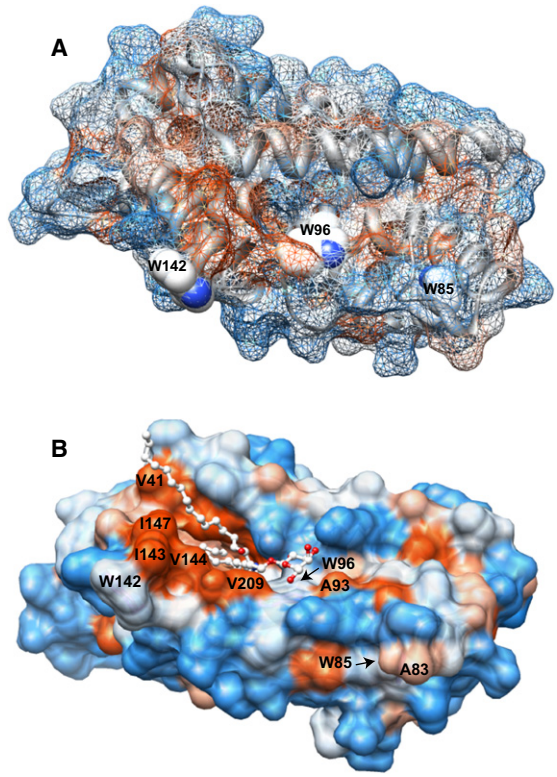

FIGURE 1 Tryptophan topography and surface hydrophobicity of human GLTP. Mapping was accomplished using Chimera, which relies on the Kyte-Doolittle scale to rank amino acid hydrophobicity, with blue indicating most hydrophilic, white equaling 0.0, and orange-red being most hydrophobic. (*A*) Structure of the glycolipid-free form of human GLTP (PDB 1SWX). (*B*) Structure of human GLTP complexed with *N*-nervonoyl GalCer (PDB 2EUK).

(Fig. 2 *A* and Table S1) and characterized by a highly cooperative, thermally induced unfolding transition near 54°C (Fig. 2 *C*). The findings are consistent with high-resolution x-ray diffraction analyses showing a two-layer fold dominated by α-helices and lacking disulfide stabilization (4–6). As illustrated in Fig. 2 *A* and Table S1, the overall secondary structures of the three Trp mutants, i.e., W96Y-GLTP, W96F-W142Y-GLTP, and W85Y-W96F-GLTP also are dominated by α-helices, albeit 6–11% less than in wtGLTP, and are characterized by unfolding transition temperatures of 55.6, 52.5 and 49°C, respectively. W85Y-W96F-GLTP showed slightly greater loss of helicity reflected by an average shortening of helices by approximately one residue (or loss of one entire helix) and a stability decrease of ~5°C.

Near-UV-CD (250–350 nm) analyses enable potential insights into local tertiary structure (21–23). Signals in the 250–270 nm region generally are attributed to Phe, those in the 270–290 nm region to Tyr, and those in the 280–300 nm region to Trp. As shown in Fig. 2 *B*, near-UV-CD spectra of wtGLTP are characterized by low environmentally induced optical activity emanating from the aromatic residues, i.e., 3 Trp, 10 Tyr, and 10 Phe. The negative signals at ~255, ~262, and ~268 nm belong to the 10 Phe residues, whereas

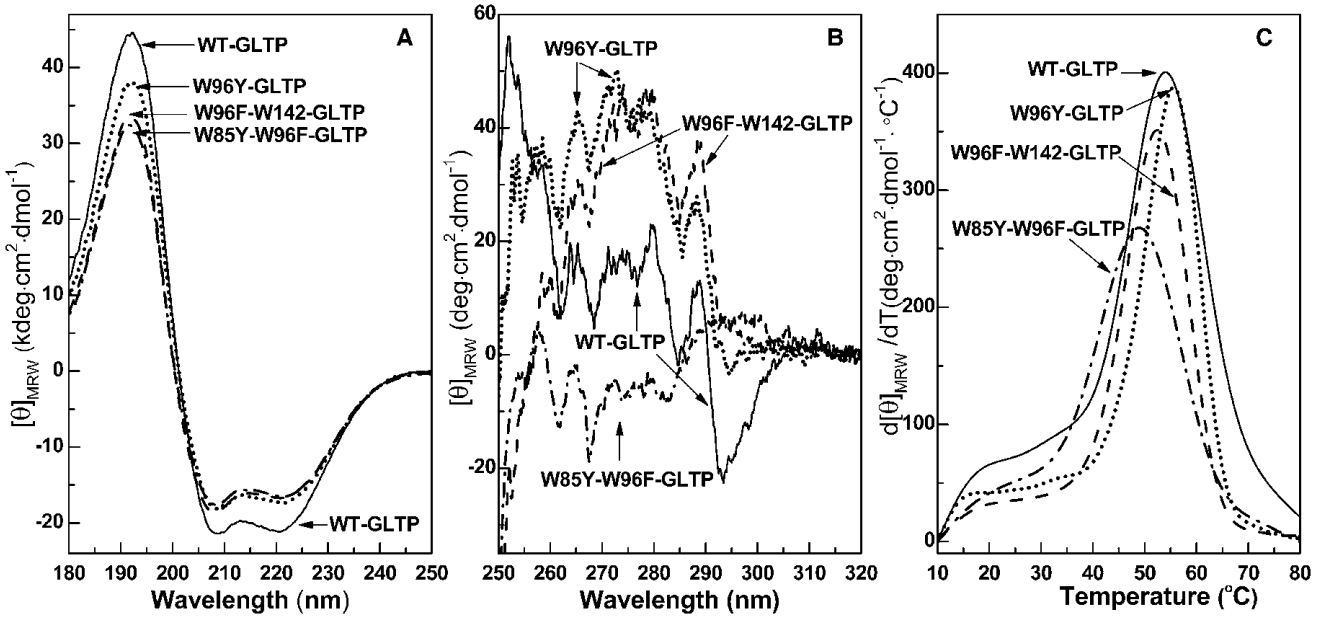

FIGURE 2 CD spectra of wtGLTP and Trp^{96}-less mutants. (*A*) Far-UV CD. The spectra are characteristic of high helical content in GLTP with large negative n-π* transitions at 222 nm and π-π* transitions split into two transitions because of exciton coupling resulting in negative bands at ~208 nm and positive bands at ~192 nm. (*B*) Near-UV CD. For wtGLTP and the three Trp^{96}-less mutants, the near-UV CD signals are weak. The loss of the negative 293-nm signal in all three mutants suggests that it originates from Trp^{96}. (*C*) Derivative plots for temperature dependence of molar ellipticity at 222 nm. The relatively low midpoints of all unfolding transitions are consistent with a lack of conformational stabilization by intramolecular disulfides, as expected for the GLTP fold. The W85Y-W96F-GLTP conformation is the most strongly destabilized ($T_m = 49°C$), whereas W96Y-GLTP ($T_m = 55.6°C$) stability slightly exceeds that of wtGLTP ($T_m = 54°C$). For W96F-W142Y-GLTP, $T_m = 52.5°C$. For details of spectrum recording, see Supporting Material.

the prominent negative signal near 293 nm can originate from Tyr or Trp. W96Y-GLTP and W96F-W142Y-GLTP show a moderate increase in the Trp/Tyr signal region, whereas W85Y-W96F-GLTP spectra are least similar to wtGLTP. The loss of the negative 293-nm signal in all three mutants suggests that it originates from W96.

3D modeling of GLTP Trp mutants

The tertiary structure of each mutant also was analyzed using the 3D-Jigsaw Comparative Modeling algorithm, which builds three-dimensional protein models based on homologs of known structure (24). The analyses indicate that the Trp point mutations exert minimal effects on the global tertiary folding of GLTP (Fig. S2).

Steady-state fluorescence analysis

Fig. 3 shows the Trp emission responses of wtGLTP, W96Y-GLTP, W85Y-W96F-GLTP, and W96F-W142Y-GLTP at identical protein concentrations. The spectra allow estimation of the relative contribution of each Trp to the total average signal of wtGLTP, showing that W96, W142, and W85 contribute ~70–80%,~16–20%, and ~4–5%, respectively. The high intensity of W96 is consistent with partially limited accessibility compared to the moderate intensity of W142, which is totally accessible to the polar aqueous milieu (25). The low intensity of the W85 emission seems to reflect quenching of its indole ring by sandwiching between P86 and K78 (cation-π interaction). The λ_{max} values of 345 nm for W96Y-GLTP, 346 nm for W85Y-W96F-GLTP, and 336 nm for W96F-W142Y-GLTP also are consistent with greater exposure of W96 and W142 to the aqueous milieu compared to W85.

Quantum yields and lifetimes

Compared to wtGLTP, elimination of W96, W96 + W85, and W96 + W142 decreased the quantum yields by ~64%, ~68%, and ~92%, respectively (Table 1). Mean lifetimes of 6.71, 5.51, 4.44, and 3.26 ns for wtGLTP, W96Y-GLTP, W85Y-W96F-GLTP, and W96F-W142Y-GLTP, respectively, followed a similar hierarchy.

Quenching of wtGLTP and Trp mutants with soluble quenchers

Trp exposure was analyzed using acrylamide and KI to quench Trp emission. Fig. 4 *A* shows the quenching profiles obtained for wtGLTP and Trp^{96}-less GLTP mutants with respect to acrylamide concentration. The slopes of the Stern–Volmer quenching constants yielded K_{SV} values (Table 2) of 5.89, 6.35, 7.51, and 2.67 M^{-1} for wtGLTP, W96Y-GLTP, W85Y-W96F-GLTP, and W96F-W142Y-GLTP, respectively. Quenching profiles obtained with iodide were nearly linear for wtGLTP but showed downward

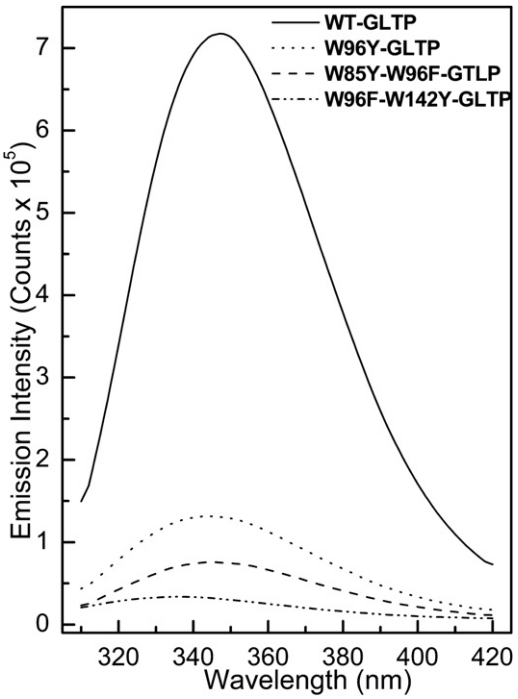

FIGURE 3 Trp emission of wild-type GLTP and Trp[96]-less mutants. Emission spectra of W96Y-GLTP, W85Y-W96F-GLTP, and W96F-W142Y-GLTP were obtained in phosphate-buffered saline at pH 7.4 by exciting at 295 nm as described in the Supporting Material.

curvature with Trp[96]-less GLTP mutants, especially above 150 mM KI. For this reason, the corresponding average rate constant for collisional quenching (k_q) by acrylamide and KI, also was calculated ($k_q = K_{sv}/\tau_o$, where τ_o is the average lifetime of fluorescence decay) and listed in Table 2. Among the Trp[96]-less GLTP mutants, k_q and K_{SV} values were consistent with greater quencher access to W142 compared to W85.

Red-edge excitation shift analyses

Solvent accessibility and environmental mobility for each Trp were further analyzed by measuring the emission λ_{max} after excitation at different wavelengths along the red edge of the Trp absorption spectrum. Increases in emission λ_{max}, known as red-edge excitation shifts (REES) (26,27), can indicate environmental heterogeneity reflecting polarity change in the vicinity of Trp and/or restricted Trp mobility. Fig. 5 shows that changing the excitation wavelength from

TABLE 1 Quantum yields of wtGLTP and Trp mutants of wtGLTP at 25°C

Protein	Average quantum yield	Mean lifetime
wtGLTP	0.207 (±0.004)	6.71 ns
W96Y-GLTP	0.0747 (±0.002)	5.51 ns
W85Y-W96F-GTLP	0.0677 (±0.003)	4.44 ns
W96F-W142Y-GLTP	0.0178 (±0.0003)	3.26 ns

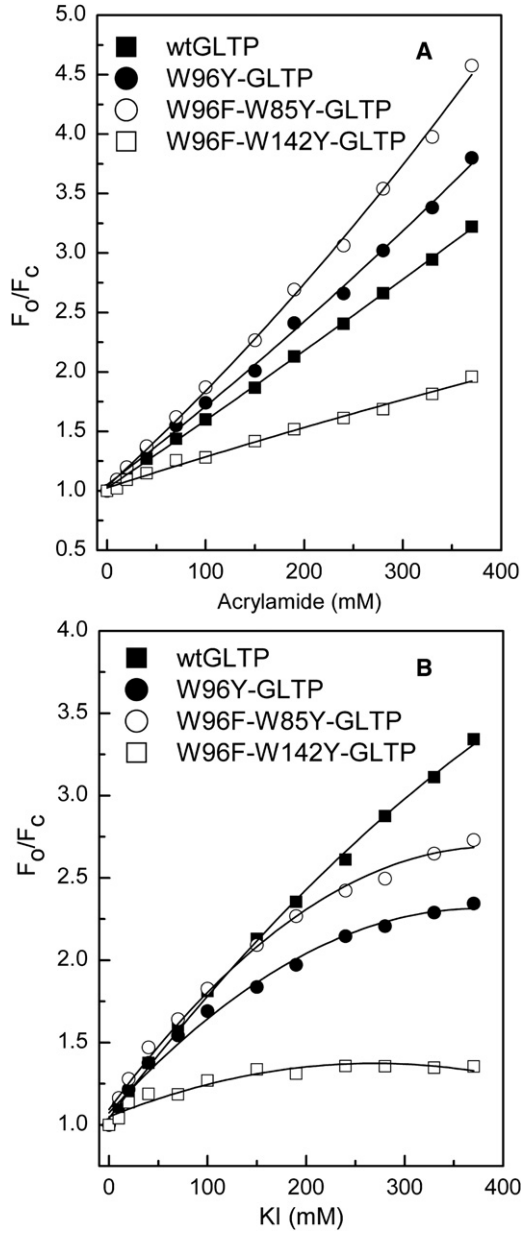

FIGURE 4 Acrylamide and KI quenching of wtGLTP and Trp[96]-less GLTP mutants Evaluated according to Stern-Volmer. (A&B) Protein samples in PBS were titrated with small aliquots of 5M stock quencher solution and fluorescence spectra were recorded after each addition. KI stock solution was stabilized with 10 mM sodium thiosulfate to prevent the formation of I_3^-, which absorbs in the region of Trp fluorescence. Stern-Volmer quenching constants (K_{sv}) were determined by nonlinear fitting and were used to calculate collisional quenching rate constants (k_q) according to $k_q = K_{sv}/\tau_o$. Values are listed in Table 2.

280 nm to 307 nm for wtGLTP results in λ_{max} shifts from 347 to 345 nm, indicating no REES. Use of excitation wavelengths $\geq$290 nm to minimize contributions from the 10 Tyr residues of wtGLTP did not change the outcome. For W96Y-GLTP, W85Y-W96F-GLTP, and W96F-W142Y-GLTP, similar emphasis on excitation wavelengths $\geq$290 nm resulted in REES of ~4 nm, ~3 nm, and >12 nm, respectively.

TABLE 2 Trp emission quenching analysis

Protein	Acrylamide		KI	
	K_{sv}	$k_q \times 10^{-9}$	K_{sv}	$k_q \times 10^{-9}$
wtGLTP	5.89	0.8775	7.88	1.175
W96Y-GLTP	6.35	1.152	6.58	1.194
W85Y-W96F-GLTP	7.51	1.692	8.16	1.837
W96F-W142Y-GLTP	2.67	0.819	2.41	0.739

K_{sv}, Stern-Volmer constant; k_q, collisional quenching rate constant.

REES induced by membrane interaction

Motional restriction of a polar fluorophore by ligand binding or by penetration into lipid phases can produce REES when the dipolar relaxation time of the solvent shell around the fluorophore becomes equal to or longer than the fluorescence lifetime (26,27). Fig. 6 and Fig. S4 show that wtGLTP exhibited an ~1–2 nm free-solution REES value that remained low in the presence of palmitoyloleoylphosphatidylcholine (POPC) vesicles but increased substantially (6–7 nm) when the POPC vesicles contained glycolipid. With Trp^{96}-less mutants, substantial REES was observed in the absence of vesicles if either W85 or W142 was replaced. For instance, W85Y-W96F-GLTP showed 8–11 nm REES in the absence or presence of POPC vesicles lacking or containing glycolipid. W96F-W142Y-GLTP behaved similarly, except that higher REES (17–23 nm) was observed. The lack of membrane-induced REES for the Trp double mutants raised the possibility that replacement of W96 might hinder detection of membrane-induced changes. However, mutation of W96 to either Y or F resulted in relatively low REES in solution but significantly elevated REES in the presence of POPC vesicles. W96Y-GLTP exhibited a 4-nm REES that increased significantly upon incubation with POPC vesicles lacking (~8 nm) or containing (~12 nm) glycolipid. A similar response was observed with W96F-GLTP (data not shown). Collectively, the data suggest that the strong W96 signal obscures detection of membrane interaction (but not glycolipid binding) and that both W85 and W142 are needed in Trp^{96}-less mutants to observe REES changes induced by membrane interaction.

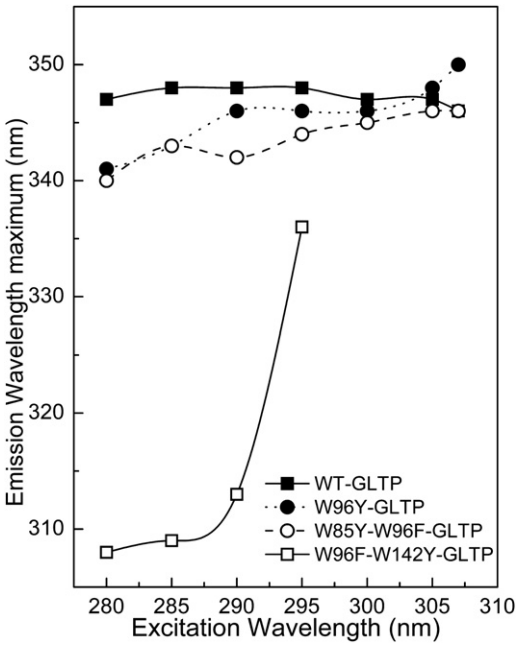

FIGURE 5 REES dependence of Trp emission maxima of Trp^{96}-less GLTP mutants. Fluorescence measurements were performed as described in the Supporting Material. Protein concentrations were 1 μM.

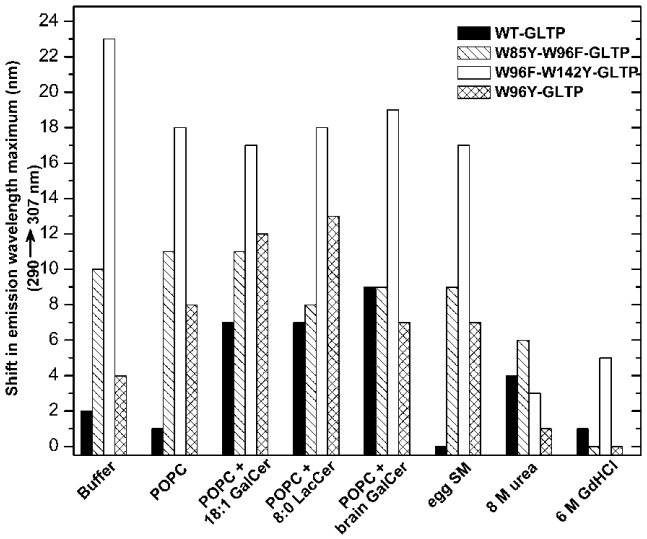

FIGURE 6 REES of wtGLTP and GLTP Trp^{96}-less mutants in the presence of various lipids. Fluorescence measurements were performed as described in the Supporting Material. Determinations for W96F-W142Y-GLTP were limited to excitations of 295 nm or less because of the extremely weak emission signal peak. To minimize contributions from Tyr, data were analyzed from excitations of 290 nm and higher. Protein concentrations were 1 μM.

Membrane effects on fluorescence lifetimes and time-resolved anisotropy Decays

To evaluate further, lifetimes were determined in the presence of POPC or POPC/C8-LacCer (8:2) vesicles. Slightly shortened lifetimes were observed for wtGLTP (6.71→6.41 ns) and W85Y-W96F-GLTP (4.44→4.32 ns) upon incubation with POPC vesicles, whereas slightly longer lifetimes resulted for W96Y-GLTP (5.51→5.63 ns) and W96F-W142Y-GLTP (3.26 →3.41 ns). When LacCer was included in the POPC vesicles, wtGLTP (6.71→ 4.74 ns) and W96Y GLTP (5.51→4.36 ns) displayed substantially shorter lifetimes (30%↓ and 20%↓, respectively), whereas the W85Y-W96F-GLTP liftetime was unchanged (4.44→4.38 ns) and that of W96F-W142Y-GLTP was slightly longer (3.26→3.5 ns). Table S2 summarizes the lifetime data and also contains the calculated rotational correlation times, which were found to be 15.6, 14.97, 16.11, and 16.34 ns for wtGLTP, W96Y-GLTP, W85Y-W96F-GLTP,

and W96F-W142Y-GLTP, respectively, in the absence of vesicles. Values of 15.48, 12.09, 8.89, and 5.91 ns, respectively, were determined in the presence of POPC vesicles, compared to values of 6.37, 8.73, 4.79, and 3.83 ns when the vesicles contained LacCer. The data show that all three Trp residues undergo dynamic changes during interaction with membranes containing glycolipid. Although the changes associated with W96 reflect glycolipid binding, those of W142 and W85 are consistent with environmental and/or conformational changes that occur in response to membrane interaction.

Emission-intensity changes induced by membrane interaction

Fig. 7 shows how incremental addition of POPC vesicles (0–110 μM) lacking or containing 20 mol % 8:0-LacCer affected the emission intensity of the Trp^{96}-less mutants. WtGLTP, which served as a reference (Fig. 7 *A*), showed a large λ_{max} blue shift, i.e., ~347→336 nm, accompanied by substantially decreased (~40%) emission intensity upon addition of sufficient glycolipid (~6–8 μM vesicles) to saturate the single glycolipid binding site. Further additions of vesicles produced small decreases in intensity along with slightly more blue-shifting of λ_{max} (~2–3 nm). In contrast, when the POPC vesicles lacked glycolipid (Fig. 7 *A*, *left*), the decreases in Trp emission intensity and λ_{max} blue shift occurred incrementally over the entire range of vesicle additions and without the initial large changes induced by glycolipid binding. The net effect was less intensity decline (~15%) and almost no λ_{max} blue shift (~1 nm). From these responses, the membrane partition coefficient values of wtGLTP were calculated as for the fungal GLTP, HET-C2 (28). wtGLTP partition coefficients were calculated to be 10.3 and 22.2 μM for POPC small unilamellar vesicles (SUVs) and POPC extrusion vesicles, respectively; whereas the respective K_d values were 1.43 and 3 μM with SUVs and extrusion vesicles containing LacCer (Table 3).

Compared to wtGLTP, all three Trp^{96}-less mutants exhibited different changes in Trp emission upon stepwise addition of membrane vesicles containing or lacking

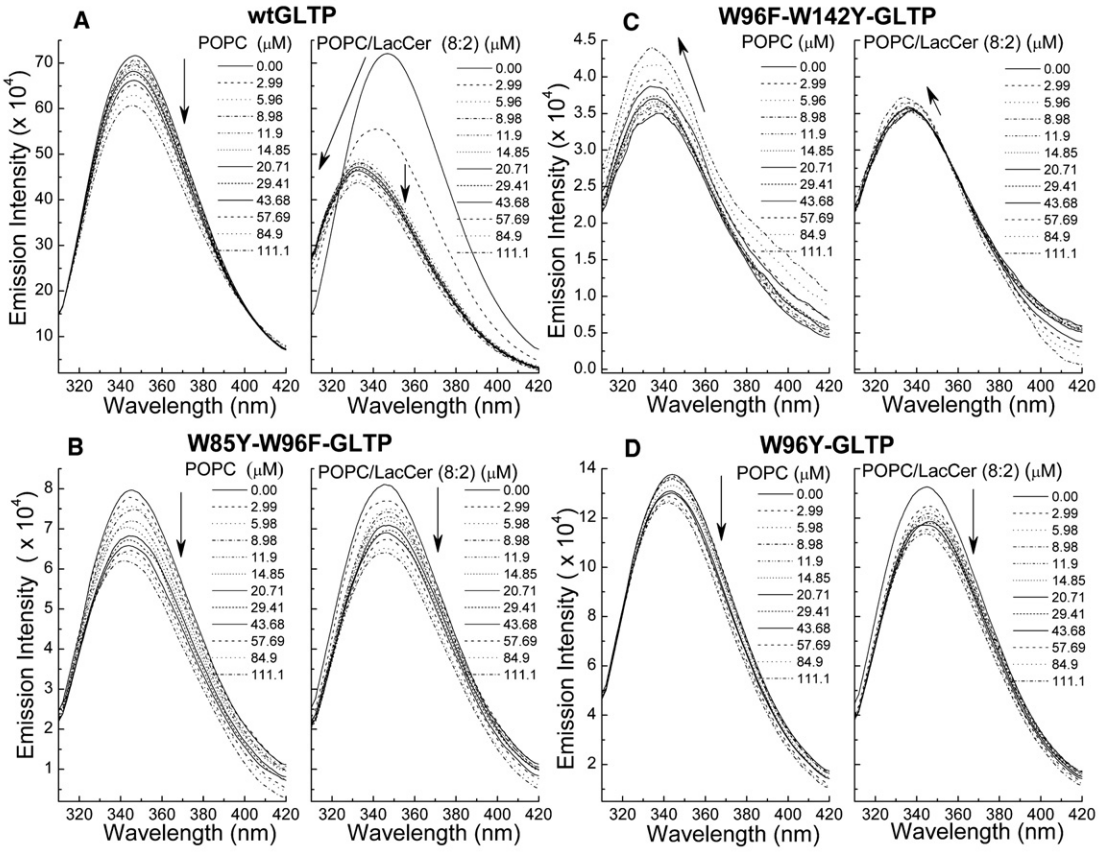

FIGURE 7 Changes in Trp emission of wtGLTP and Trp^{96}-less mutant induced by lipids. POPC vesicles lacking or containing glycolipid were introduced in stepwise fashion with 5-min incubation times between injections. (*A*) Wt-GLTP. The initial aliquots of membrane vesicles containing LacCer induce a strong intensity decrease and λ_{max} blue shift in wtGLTP (by ninth aliquot, total available glycolipid = ~1.35 μM). Additional injections result in Trp emission intensity decreases of similar magnitude to those observed with POPC vesicles lacking glycolipid. The λ_{max} blue shift occurred only when the vesicles contained glycolipid. (*B*) W85Y-W96F-GLTP. (*C*) W96F-W142Y-GLTP. (*D*) W96Y-GLTP were treated the same as in *A*. Fluorescence experiments were performed as detailed in the Supporting Material.

TABLE 3 K_d values of WT-GLTP and Trp mutants for SUV and extruded vesicles

	Partition coefficient (K_d) (μM)			
	POPC		C8-LacCer/POPC	
Protein	SUV	Extruded vesicles	SUV	Extruded vesicles
WtGLTP	10.31 ± 0.29	22.21 ± 4.73	1.43 ±0.07	3.05 ±0.65
W96Y-GLTP	—	—	2.11 ±0.14	1.04 ±0.16
W85-W96F-GLTP	4.13 ± 0.24	6.61 ±1.07	4.88 ±0.58	7.59 ±1.28
W96F-W142Y-GLTP	—	—	—	—

Partition coefficient constants (K_d) were determined by nonlinear fitting analyses of POPC- and C8-LacCer/POPC-vesicle-induced changes in GLTP Trp emission intensity, as detailed in the Supporting Material. For C8-LacCer/POPC, values were calculated at fixed wavelength (353 nm) in the emission peak for wtGLTP (12). Glycolipid pool size in the POPC-vesicle outer leaflet and available for interaction with GLTP was estimated from transbilayer distributions as described previously (12).

glycolipid (Fig. 7, *B–D*). As expected, the decreases in emission intensity and the λ_{max} blue shifts were strongly diminished in absolute terms, consistent with the dominating contributions by W96 (12). The weakness of the signal changes and lack of clear-cut saturation compromised accurate assessment of membrane partition coefficients for W96Y and W96F-W142Y-GLTP, but not for W85Y-W96F-GLTP (Table 3). It is worth noting, however, that stepwise addition of POPC vesicles either lacking or containing 8:0 LacCer to W96Y-GLTP (Fig. 7 *D*) resulted in emission-intensity decreases that are larger in magnitude when glycolipid is present in the vesicles. A small blue shift (~2 nm) in λ_{max} also occurs. The finding is consistent with W142 and/or W85 providing relatively weak signal change that reflects protein partitioning to POPC vesicles. To determine whether W142 or W85 was responsible, additional experiments were performed. Stepwise addition of POPC vesicles either lacking or containing 8:0 LacCer to the GLTP mutant containing only W142 (W85Y-W96F-GLTP (Fig. 7 *B*)) resulted in comparable decreases in relative intensity, except for the initial additions. Also, little or no λ_{max} blue shift was evident (Table S3). When only W85 remained (W96F-W142Y-GLTP (Fig. 7 *C*)), increases in relative emission intensity were elicited by stepwise addition of POPC vesicles. It is worth noting that when vesicles lacked glycolipid, larger intensity increases and a significantly blue-shifted λ_{max} were observed.

DISCUSSION

Protein classification as peripheral and amphitropic originally indicated weak and reversible binding to membranes, with protein function dependent on the translocation process (29). More recently, the amphitropic protein category has been expanded to include water-soluble, channel-forming polypeptide toxins, despite the fact that functional channel formation by the peptides results in irreversible membrane association, a key feature of integral membrane proteins (30). GLTP meets the original criteria of a peripheral, amphitropic protein by virtue of transient membrane association during the binding and transfer of glycolipids. More important, from the standpoint of conformational architecture among known membrane interaction domains and lipid binding motifs, the GLTP fold is unique.

In vertebrate GLTPs, all three Trp residues are conserved (3). Although the key role of Trp^{96} in the glycolipid binding process has been unequivocally established (4–6,12,19), the involvement of the Trp residues in membrane interaction and other events has remained less clear. Various reports have suggested that one, two, or all three of the Trps are part of a putative GLTP membrane interaction domain (9–11). Our approach for defining W85 and W142 functionality involved an atypical point mutation strategy for Trp double-mutant construction. Rather than using only Phe as a replacement for Trp, our strategy relied on replacement of Trp with both Phe and Tyr. Previously, West et al. (10) used the standard Phe-only substitution approach to generate double-Trp mutants, W96,142F-GLTP and W85,96F-GLTP, but found them to be inactive, thus preventing functional assessment of W85 and W142. Our atypical mutational strategy resulted in active GLTP double-Trp mutants that contain only W85 or W142.

The success of the mutational strategy emphasizes how seemingly minor structural differences in aromatic side chains can be important for maintaining physicochemical features essential for functionality. Like Trp, Tyr is somewhat polar by virtue of a hydroxyl group at the *para* position of the benzene ring, whereas Phe is very nonpolar, having hydrogen at the same position of its benzene ring. In human GLTP, the increased polarity provided by Tyr substitution is expected to help maintain favorable energetics among neighboring residues that interact with W85 and W142. In the case of W142, the effectiveness of Tyr over Phe seems to support this idea. W142 is completely exposed on the protein surface in an ideal position for penetrating the bilayer interfacial region during membrane interaction by GLTP (4,13,31–34). Although located sufficiently close (~4.6 Å) to K146 for cation-π interaction (35), our crystal structures indicate less-than-optimal orientations (Fig. 8, *A* and *B*), leaving the issue unresolved. More likely, mutation of W142 to Phe, when also accompanied by mutation of Trp^{96} to Phe (as studied by West et al. (10)), enhances self-aggregation (and activity loss) compared to W96F-W142Y-GLTP. Phe residues are known to promote

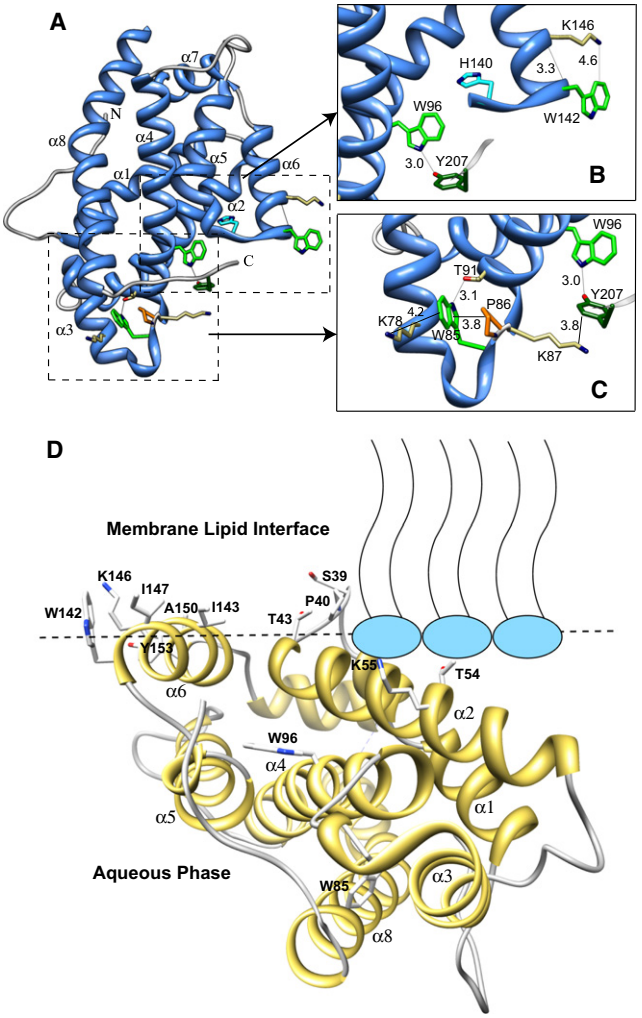

FIGURE 8 Neighboring residues of Trp^{85} and Trp^{96} in GLTP. (*A–C*) Trp^{85} is near the surface but its indole ring projects inward and is sandwiched between Pro^{86} and Lys^{78}, which is suitably located for cation-π interaction with Trp^{85} (35). Trp^{96} is surface-localized and completely accessible to the aqueous milieu. Nearby Lys^{146} does not appear to be optimally oriented for cation-π interaction with Trp^{96}. Trp^{85} is located ~30–32 Å from Trp^{142} and ~14–16 Å from Trp^{96}. (*D*) GLTP orientation and positioning during initial membrane docking. Residues involved in the initial docking of GLTP with the membrane interface were identified using the orientation of proteins in membranes (OPM) computational approach (34). Lipid molecules, comprising half of the membrane (*aqua*), are shown with wavy lines to represent the lipid hydrocarbon chains. The dotted line corresponds to the membrane interface. GLTP helices (*gold*) and important side-chain residues are labeled.

protein-protein interactions including self-interaction (36). The presence of two nonpolar Phe residues on the GLTP surface within its membrane-interaction patch may be simply too much, given the preponderance of neighboring nonpolar residues (Fig. 1 and Fig. S5).

In the case of W85, stacking occurs against *cis*-Pro^{86} (~3.8 Å) along with a favorable cation-pi interaction (~4.2 Å) with K78 (Fig. 8 *C*). This sandwiching of the indole ring facilitates hydrogen bonding (~3.1 Å) between the pyrrole nitrogen group and the Thr^{91} side-chain hydroxyl group, accounting for the large REES and highly quenched state of W85 in GLTP. Favorable stacking energetics between Trp and *cis*-Pro occur because of the dipole originating with the nitrogen heteroatom and the cyclic arrangement of proline, resulting in favorable electrostatic interaction (37,38). Similarly, because of favorable stacking, Tyr occurs more frequently than Phe immediately before *cis*-Pro in native proteins (39). As for cation-π interactions (35), the likelihood of aromatic side-chain participation is Trp > Tyr > Phe, providing a rationalization for better preservation of function by mutation to Tyr than by mutation to Phe.

Distinct functional roles for the three Trps of the vertebrate GLTP fold

Since all three Trp^{96}-less mutants show preservation of glycolipid transfer activity (Fig. S1), it is not surprising that far-UV CD shows helical content remaining high and temperature midpoints of thermally-induced unfolding transition differing only slightly from those for wtGLTP (~54°C). For W96F-W142Y-GLTP and W85Y-W96F-GLTP, unfolding-transition temperature midpoints are 52.5 and 49°C, respectively, along with lower transition cooperativities, indicating slight destabilization. In contrast, the 55.6°C unfolding transition temperature midpoint and enhanced transition cooperativity of W96Y-GLTP indicate slightly increased stability. Near-UV-CD analyses (250–350 nm) proved to be less informative for assessment of tertiary folding status, despite the presence of 10 intrinsic Tyr along with Trp, because of an inherently weak near-UV CD signal. Nonetheless, fluorescence emission responses of the Trp^{96}-less mutants are consistent with preservation of global folding. Collectively, the emission λ_{max} values, the accessibility to quenching by acrylamide and iodide, and the REES of W85Y-W96F-GLTP and W96F-W142Y-GLTP suggest free accessibility and dynamic motion by W142, but limited accessibility and restricted motion of W85.

It is noteworthy that all three GLTP Trp^{96}-less mutants display dramatically reduced absolute average Trp intensities, quantum yields, and lifetimes as a consequence of Trp^{96} replacement. The mutants make it possible to estimate the signal contribution of each Trp in wtGLTP to the total average Trp intensity: ~70–80% for W96, ~16–20% for W142, and ~4–5% for W85. When the dominant emission contributions of W96 and related changes induced by glycolipid binding (i.e., the ~40% intensity decrease and ~12-nm λ_{max} blue shift (12)) are eliminated, the emission responses associated with W142 and/or W85 during membrane interaction become observable. Taking into consideration the location of W142 and its free accessibility on the surface of GLTP, the steadily declining intensity of W85Y-W96F-GLTP fluorescence (and lack of λ_{max} blue shift) in response to stepwise addition of POPC vesicles containing or lacking glycolipid provides experimental support for W142 involvement in the

GLTP-membrane interaction process, as predicted when GLTP structure was first solved (4). The lack of strongly elevated GLTP partitioning to vesicles containing glycolipid is consistent with our earlier observations by resonance energy transfer between GLTP and vesicles containing dansyl phosphatidylethanolamine at physiological ionic strength (9). The decrease in W142 emission intensity supports previous findings of shallow penetration into the outer surface of the membrane interfacial region, possibly involving cation-π interaction with the choline moiety (33,40), rather than deep penetration into the membrane hydrocarbon chain region (Fig. 8 *D*), in agreement with the study by Rao et al. showing a lack of hydrocarbon chain perturbation for wtGLTP by diphenylhexatriene fluorescence (9). In the vesicle outer surface, curvature stress alters lipid packing and increases the mobility of hydrated functional groups in the vicinity of the glyceride backbone (41), conditions expected to enhance Trp quenching. Other examples of decreases in Trp emission intensity have been reported for other proteins interacting with SUVs produced by probe sonication (42–44).

In contrast to the freely exposed environment of W142 of the α6 helix (Figs. 1 *A* and 8 *B*), W85 is located along the α3-α4 connecting ribbon, where stacking against P86 results in inward projection of the indole ring and facilitation of a cation-π interaction with K78 on the adjacent α3 helix (Fig. 8 *C*). Van der Waals bridging contacts between V88 (also on the α3-α4 connector) and Y81 (on the α3 helix) further stabilize the sharp switchback loop in this same region. The enhanced sensitivity of W96F-W142Y-GLTP to thermal destabilization compared to all other mutants and wtGLTP (Fig. 2 *C*) leads us to conclude that the role of the buried and tightly sandwiched Trp^{85} is to help maintain proper GLTP folding and stability. It is tempting to speculate that the intensity increase and λ_{max} blue shift of W96F-W142Y that accompany the stepwise addition of vesicles lacking glycolipid reflect a gate-opening conformational change triggered by interaction with the membrane interface. Partial relief of W85 quenching by the P86/K78 sandwiching could accompany such a conformational change during membrane interaction. The near absence of emission changes when vesicles contain glycolipid is consistent with rapid return to a conformational state similar to apoGLTP after glycolipid binding. Indeed, x-ray diffraction data show that the conformation of GLTP is globally unchanged after glycolipid binding, with only localized and limited expansion of a hydrophobic pocket encapsulating the nonpolar lipid region (4–6). It is clear that the buried nature of the Trp^{85} indole ring precludes a direct role in initiation of GLTP docking with the membrane (Fig. 8 *D*).

CONCLUSIONS

The significance of this study lies in the new insights gained into the workings of Trp^{142} (membrane interaction) and Trp^{85} (protein folding stabilization) in human GLTP compared to the known role for Trp^{96} in glycolipid binding. The findings illustrate the remarkable versatility of the three intrinsic Trp residues, each having its own primary intramolecular function within the novel, amphitropic GLTP fold.

SUPPORTING MATERIAL

Supporting material, including four tables and five figures, is available at http://www.biophysj.org/biophysj/supplemental/S0006-3495(10)01033-7.

We are grateful for financial support from the National Institute of General Medical Sciences (GM45928 and GM34847) and the National Cancer Institute (CA121493) of the National Institutes of Health, Russian Federation for Biological Research No. 09-04-00313, the Abby Rockefeller Mauzé Trust, and the Dewitt Wallace, Maloris, Mayo, and Hormel Foundations.

REFERENCES

1. Brown, R. E., and P. Mattjus. 2007. Glycolipid transfer proteins. *Biochim. Biophys. Acta.* 1771:746–760.
2. Lin, X., P. Mattjus, …, R. E. Brown. 2000. Cloning and expression of glycolipid transfer protein from bovine and porcine brain. *J. Biol. Chem.* 275:5104–5110.
3. Zou, X., T. Chung, …, R. E. Brown. 2008. Human glycolipid transfer protein (*GLTP*) genes: organization, transcriptional status and evolution. *BMC Genomics.* 9:72.
4. Malinina, L., M. L. Malakhova, …, D. J. Patel. 2004. Structural basis for glycosphingolipid transfer specificity. *Nature.* 430:1048–1053.
5. Malinina, L., M. L. Malakhova, …, D. J. Patel. 2006. The liganding of glycolipid transfer protein is controlled by glycolipid acyl structure. *PLoS Biol.* 4:e362.
6. Airenne, T. T., H. Kidron, …, T. A. Salminen. 2006. Structural evidence for adaptive ligand binding of glycolipid transfer protein. *J. Mol. Biol.* 355:224–236.
7. D'Angelo, G., E. Polishchuk, …, M. A. De Matteis. 2007. Glycosphingolipid synthesis requires FAPP2 transfer of glucosylceramide. *Nature.* 449:62–67.
8. Halter, D., S. Neumann, …, H. Sprong. 2007. Pre- and post-Golgi translocation of glucosylceramide in glycosphingolipid synthesis. *J. Cell Biol.* 179:101–115.
9. Rao, C. S., T. Chung, …, R. E. Brown. 2005. Glycolipid transfer protein interaction with bilayer vesicles: modulation by changing lipid composition. *Biophys. J.* 89:4017–4028.
10. West, G., M. Nylund, …, P. Mattjus. 2006. Membrane interaction and activity of the glycolipid transfer protein. *Biochim. Biophys. Acta.* 1758:1732–1742.
11. Neumann, S., M. Opacić, …, M. R. Egmond. 2008. Glycolipid transfer protein: clear structure and activity, but enigmatic function. *Adv. Enzyme Regul.* 48:137–151.
12. Zhai, X., M. L. Malakhova, …, R. E. Brown. 2009. Glycolipid acquisition by human glycolipid transfer protein dramatically alters intrinsic tryptophan fluorescence: insights into glycolipid binding affinity. *J. Biol. Chem.* 284:13620–13628.
13. Mattjus, P. 2009. Glycolipid transfer proteins and membrane interaction. *Biochim. Biophys. Acta.* 1788:267–272.
14. Cho, W., and R. V. Stahelin. 2005. Membrane-protein interactions in cell signaling and membrane trafficking. *Annu. Rev. Biophys. Biomol. Struct.* 34:119–151.
15. Hurley, J. H. 2006. Membrane binding domains. *Biochim. Biophys. Acta.* 1761:805–811.
16. Cho, W. (editor). 2006. Lipid-binding domains. *Biochim. Biophys. Acta* (*Special Issue: Lipid-Binding Domains*). 1761:803–968.

17. Lemmon, M. A. 2008. Membrane recognition by phospholipid-binding domains. *Nat. Rev. Mol. Cell Biol.* 9:99–111.

18. Malakhova, M. L., L. Malinina, …, R. E. Brown. 2005. Point mutational analysis of the liganding site in human glycolipid transfer protein. Functionality of the complex. *J. Biol. Chem.* 280:26312–26320.

19. Li, X.-M., M. L. Malakhova, …, R. E. Brown. 2004. Human glycolipid transfer protein: probing conformation using fluorescence spectroscopy. *Biochemistry.* 43:10285–10294.

20. Rao, C. S., X. Lin, …, R. E. Brown. 2004. Glycolipid transfer protein mediated transfer of glycosphingolipids between membranes: a model for action based on kinetic and thermodynamic analyses. *Biochemistry.* 43:13805–13815.

21. Venyaminov, S. Y., E. S. Klimtchuk, …, T. A. Craig. 2004. Changes in structure and stability of calbindin-D$_{(28K)}$ upon calcium binding. *Anal. Biochem.* 334:97–105.

22. Craig, T. A., L. M. Benson, …, R. Kumar. 2006. Metal-binding properties of human centrin-2 determined by micro-electrospray ionization mass spectrometry and UV spectroscopy. *J. Am. Soc. Mass Spectrom.* 17:1158–1171.

23. Kelly, S. M., T. J. Jess, and N. C. Price. 2005. How to study proteins by circular dichroism. *Biochim. Biophys. Acta.* 1751:119–139.

24. Bates, P. A., L. A. Kelley, …, M. J. Sternberg. 2001. Enhancement of protein modeling by human intervention in applying the automatic programs 3D-JIGSAW and 3D-PSSM. *Proteins.* 5 (*Suppl 5*):39–46.

25. Lakowicz, J. R. 2006. Principles of Fluorescence Spectroscopy, 3rd ed. Springer, New York.

26. Demchenko, A. P. 2002. The red-edge effects: 30 years of exploration. *Luminescence.* 17:19–42.

27. Raghuraman, H., D. A. Kelkar, and A. Chattopadhyay. 2005. Novel insights into protein structure and dynamics utilizing the red edge excitation shift approach. *In* Reviews in Fluorescence 2005. C. D. Geddes, and J. R. Lakowicz, editors. Springer, New York. 199–222.

28. Kenoth, R., D. K. Simanshu, …, R. E. Brown. 2010. Structural determination and tryptophan fluorescence of heterokaryon incompatibility C2 protein (HET-C2), a fungal glycolipid transfer protein (GLTP), provide novel insights into glycolipid specificity and membrane interaction by the GLTP fold. *J. Biol. Chem.* 285:13066–13078.

29. Johnson, J. E., and R. B. Cornell. 1999. Amphitropic proteins: regulation by reversible membrane interactions (review). *Mol. Membr. Biol.* 16:217–235.

30. Tamm, L. K. 2005. Protein-Lipid Interactions: From Membrane Domains to Cellular Networks. Wiley-VCH, Weinheim, Germany.

31. Yau, W.-M., W. C. Wimley, …, S. H. White. 1998. The preference of tryptophan for membrane interfaces. *Biochemistry.* 37:14713–14718.

32. Sanderson, J. M., and E. J. Whelan. 2004. Characterisation of the interactions of aromatic amino acids with diacetyl phosphatidylcholine. *Phys. Chem. Chem. Phys.* 6:1012–1017.

33. Esbjörner, E. K., C. E. B. Caesar, …, B. Nordén. 2007. Tryptophan orientation in model lipid membranes. *Biochem. Biophys. Res. Commun.* 361:645–650.

34. Lomize, A. L., I. D. Pogozheva, …, H. I. Mosberg. 2007. The role of hydrophobic interactions in positioning of peripheral proteins in membranes. *BMC Struct. Biol.* 7:44.

35. Gallivan, J. P., and D. A. Dougherty. 1999. Cation-π interactions in structural biology. *Proc. Natl. Acad. Sci. USA.* 96:9459–9464.

36. Yoder, N. C., and K. Kumar. 2006. Selective protein-protein interactions driven by a phenylalanine interface. *J. Am. Chem. Soc.* 128:188–191.

37. Biedermannova, L., K. E Riley, …, J. Vondrasek. 2008. Another role of proline: stabilization interactions in proteins and protein complexes concerning proline and tryptophane. *Phys. Chem. Chem. Phys.* 10:6350–6359.

38. Exarchos, K. P., T. P. Exarchos, …, D. I. Fotiadis. 2009. Detection of discriminative sequence patterns in the neighborhood of proline cis peptide bonds and their functional annotation. *BMC Bioinformatics.* 10:113.

39. Lorenzen, S., B. Peters, …, C. Frommel. 2005. Conservation of *cis* prolyl bonds in proteins during evolution. *Proteins.* 58:589–595.

40. Gaede, H. C., W.-M. Yau, and K. Gawrisch. 2005. Electrostatic contributions to indole-lipid interactions. *J. Phys. Chem. B.* 109:13014–13023.

41. Sỳkora, J., P. Jurkiewicz, …, M. Hof. 2005. Influence of the curvature on the water structure in the headgroup region of phospholipid bilayer studied by the solvent relaxation technique. *Chem. Phys. Lipids.* 135:213–221.

42. Joseph, M., and R. Nagaraj. 1995. Conformations of peptides corresponding to fatty acylation sites in proteins. A circular dichroism study. *J. Biol. Chem.* 270:16749–16755.

43. Christiaens, B., S. Symoens, …, S. Vanderheyden. 2002. Tryptophan fluorescence study of the interaction of penetratin peptides with model membranes. *Eur. J. Biochem.* 269:2918–2926.

44. Chowdary, T. K., B. Raman, …, ChM. Rao. 2007. Interaction of mammalian Hsp22 with lipid membranes. *Biochem. J.* 401:437–445.